

Unequal Mass Binary Black Hole Plunges and Gravitational Recoil

Frank Herrmann

Center for Gravitational Wave Physics
Institute for Gravitational Physics and Geometry
Penn State University, University Park, PA 16802

Ian Hinder

Center for Gravitational Wave Physics
Institute for Gravitational Physics and Geometry
Penn State University, University Park, PA 16802

Deirdre Shoemaker

Center for Gravitational Wave Physics
Institute for Gravitational Physics and Geometry
Penn State University, University Park, PA 16802

Pablo Laguna

Center for Gravitational Wave Physics
Institute for Gravitational Physics and Geometry
Penn State University, University Park, PA 16802

Abstract. We present results from fully nonlinear simulations of unequal mass binary black holes plunging from close separations well inside the innermost stable circular orbit with mass ratios $q \equiv M_1/M_2 = \{1, 0.85, 0.78, 0.55, 0.32\}$, or equivalently, with reduced mass parameters $\eta \equiv M_1 M_2 / (M_1 + M_2)^2 = \{0.25, 0.248, 0.246, 0.229, 0.183\}$. For each case, the initial binary orbital parameters are chosen from the Cook-Baumgartner equal-mass ISCO configuration. We show waveforms of the dominant $\ell = 2, 3$ modes and compute estimates of energy and angular momentum radiated. For the plunges from the close separations considered, we measure kick velocities from gravitational radiation recoil in the range 25-82 km/s. Due to the initial close separations our kick velocity estimates should be understood as a lower bound. The close configurations considered are also likely to contain significant eccentricities influencing the recoil velocity.

PACS numbers: 04.25.Dm, 04.30.Db, 04.70.Bw, 95.30.Sf, 97.60.Lf

1. Introduction

The Laser Interferometer Space Antenna (LISA) will offer a unique look at merging supermassive black holes (BHs) [3, 4]. When galaxies collide, the BHs at the center of each galaxy [5, 6] will merge and radiate gravitational waves. In a generic merger situation, the colliding BHs will have different masses and spins, thus they will radiate gravitational waves anisotropically. This anisotropic radiation will carry both a net angular and linear momentum [7]. The linear momentum emitted implies a recoil of, or kick to, the BH product of the merger. A large enough recoil may cause the BH resulting from the merger to be strongly offset from the center of the galaxy or potentially even kicked out of small galaxies [8, 9]. Such a scenario would have a significant impact on the standard picture of merger tree history of galaxies.

A complete investigation of the gravitational recoil from unequal mass BH mergers must include the contributions to the kick from the inspiral, merger and ringdown stages of the life of the binary. Given the tremendous progress that numerical relativity has recently made in simulating binary black hole (BBH) systems [10, 11, 12, 13, 14, 15], fully numerical investigations can now be used to investigate gravitational recoil. Recent numerical studies [36, 18] as well as post-Newtonian estimates [16, 17] suggest that most of the kick gets accumulated during the plunge. Motivated by these observations, we carried out a series of unequal mass BBHs simulations, using initial data that corresponds to BHs plunging from innermost stable circular orbit (ISCO), i.e. initial separations of $2.34M$. In particular, we focus on the dominant $\ell = 2, 3$ modes and study how the energy radiated in these modes changes as the mass ratio is varied. Additionally, we calculate the energy and angular momentum radiated, and from the gravitational radiation we estimate kick velocities in the range 25-82 km/s acquired by the final BH.

Soon after the completion of our study, Baker et al. [36] studied a much further separated system and Gonzales et al. [18] published fully relativistic kick estimates from BHs with initial separation of $7M$ for a broad range of mass ratios, from $q = M_1/M_2 = 1$ to $q = 0.25$, or equivalently $\eta = q/(1+q)^2$ from 0.25 to 0.16. They estimated a maximum kick of 175.70 km s^{-1} for a mass ratio of $\eta = 0.195$. Using close-limit approximation techniques Sopuerta et al. investigated gravitational wave recoil and also the effect of small eccentricities [1, 2].

Initial Data. The initial data sets are constructed via the puncture method using a spectral code [19, 20]. The essence of this method is to solve the Hamiltonian constraint for the conformal factor ϕ . The initial three-metric is conformally flat, maximally sliced, and the extrinsic curvature is given by the Bowen-York solution to the momentum constraint. The conformal factor ϕ is used to set the initial lapse as $\alpha = \phi^{-2}$ [21, 13], while the initial shift is $\beta^i = 0$.

For the equal mass setup, we evolve the so-called QC-0 initial data set [22]. This is intended to represent a quasi-circular configuration of inspiraling puncture BBHs at the ISCO. QC-0 data have been used as the starting point by other studies [11, 13, 14].

The BHs in QC-0 perform about half of an orbit prior to merging [13, 14]; that is, QC-0 looks more like a plunge/grazing collision. The intersection of the event horizon with the initial slice, however, has the topology of two separate spheres [11].

The puncture BBH data of the Bowen-York type are defined by the bare masses $m_{1,2}$ of the BHs, their coordinate locations $C_{1,2}$, assumed to be along the x -axis in the xy -plane, and their linear momentum $P_{1,2}$, pointing along the y -axis. In the construction of the initial data, we vary $m_2 = \{1, 1.2, 1.3, 2, 4\} m_1$ while keeping m_1 fixed to its QC-0 value of 0.453. We also keep fixed to the QC-0 values the puncture coordinate separation $d \equiv |C_1 - C_2| = 2.34$ and the momentum parameters $P_{1,2} = \pm 0.333$, which means that the angular momentum value, $J = 0.779$, also remains unchanged. Note that the total ADM mass, M_{ADM} , of the configurations does change as do J and P when given in ADM mass units. Due to this setup, our initial data of unequal mass BBH systems do not obey the quasi-circular orbit condition of minimal binding energy [23]. The present work is aimed at investigating the effects of varying, in the QC-0 set-up, the bare mass parameter only. The motivation behind this choice was to study gravitational recoil starting from the ISCO plunge with the simplest parameter exploration. There is strong indication that the kick imparted to the BH that has resulted from the merger is dominated by the gravitational recoil during the plunge from ISCO [16]. We are currently extending the present study and investigating both unequal mass BBH mergers with initial separations outside of ISCO in quasi-circular orbit and plunge configurations with Post-Newtonian orbital parameters [16].

Table 1 summarizes the parameters in our simulations. We list the total mass $M = M_1 + M_2$, the mass ratio parameter $\eta = M_1 M_2 / M^2$ where $M_{1,2}$ are the irreducible masses of the BHs computed from their individual apparent horizon (AH) areas, as well as angular momentum J and momentum parameter P in terms of the reduced mass, $\mu = M_1 M_2 / M$. Table 1 also provides the time t_{AH} in M_{ADM} units when a common AH is first found. For QC-0 the orbital period of the equal mass case is estimated as $t = 37.4 M_{\text{ADM}}$. The drop in the time to merger t_{AH} in our results should not be interpreted as “unequal mass binaries merge faster”. The effect is due to our approach in which the angular momentum of the configuration decreases as the bare mass ratio is decreased. Ideally one would like to compare initial data sets which are far separated and have the same orbital frequency. It is possible that for our cases with $q \leq 0.55$, a common event horizon already exists in the initial data slice; and, therefore, we are evolving a single, distorted BH.

Methods. The evolutions were carried out using a code that solves the BSSN 3+1 formulation of Einstein’s equations [24, 25, 26]. We use the “moving punctures” approach without excision [14, 13]. The code was produced by the `Kranc` code generation package [27] and uses the `Cactus` infrastructure. The simulations were performed using fourth order accurate centered finite differencing, except for the advection terms which were one-sided and second order accurate. The temporal updating is carried out with a three-step iterative Crank-Nicholson scheme with Courant factor of 0.25. Tests in the waveform for the equal-mass setup using resolutions $h = \{1/16, 1/20, 1/32\}$ produced

q	M_1/M	M_2/M	M	η	P/μ	$J/(\mu M)$	t_{AH}
1.00	0.512	0.512	1.024	0.250	1.290	2.948	18.4
0.85	0.482	0.565	1.047	0.248	1.180	2.637	12.2
0.78	0.463	0.597	1.060	0.246	1.122	2.476	9.9
0.55	0.391	0.712	1.103	0.229	0.933	1.979	5.5
0.32	0.277	0.872	1.149	0.183	0.692	1.409	2.5

Table 1. Initial data parameters and properties: The $q = 1$ case is the QC-0 data set in [22]. All models have puncture bare mass $m_1 = 0.453$, momenta $P_{1,2} = \pm 0.333$ and coordinate separation $d = 2.34$. The total mass M is given in M_{ADM} units as well as the coordinate time t_{AH} at which a common apparent horizon was found.

convergence slightly below second order. Mesh refinement in the code is provided by `Carpent` [28], and tracking of AHs is handled by `AHFinderDirect` [29].

The gauge conditions used were modified versions of the 1+log lapse and Γ -driver shifts. Specifically, the lapse α was evolved using $\partial_t \alpha = -2\alpha K$, where K is the trace of the extrinsic curvature. On the other hand, the shift vector was obtained from [14]: $\partial_t \beta^i = F B^i$ and $\partial_t B^i = \partial_t \tilde{\Gamma}^i - \beta^j \partial_j \tilde{\Gamma}^i - \xi B^i$ with ξ a constant dissipative parameter and $F = 3\alpha/4$, which guarantees that the asymptotic gauge speed associated with the longitudinal shift components is equal to the speed of light. The evolutions were started with β^i and $B^i = 0$. The advection term $\beta^j \partial_j \tilde{\Gamma}^i$ removes certain zero-speed modes of the system as analyzed in [30]. The parameter ξ can be used to tune the rate of horizon expansion over the course of the evolution; large values lead to faster horizon growth. We have used values in the range $2 \leq \xi \leq 5$ and have not found any instabilities in this range. For the runs reported in this paper we used $\xi = 4$.

Our computational domain consisted of fixed 2:1 mesh refinements with 5 levels. The finest grid spanned $-2 \leq x, y \leq 2$ and $0 \leq z \leq 2$, with the coarsest $-96 \leq x, y \leq 96$ and $0 \leq z \leq 96$ (we use bitant symmetry in the z direction). All the refinement levels except for the coarsest have the same number of grid points. We have run the unequal BBH models at two different resolutions, $h = 1/16, 1/20$.

Results. Fig. 1 shows the irreducible mass of the AHs as a function of time, where $M_{\text{irr}} = \sqrt{A/16\pi}$ and A is the AH area. In all simulations with $q > 0.32$, we are able to track very accurately M_{irr} for both of the individual merging BHs, as well as the resulting BH, over the entire course of the simulation. In the case of $q = 0.32$, we cannot track the smaller individual irreducible mass very accurately before merger. There is also a spurious drift in the common apparent horizon mass beyond the initial ADM mass content of the spacetime but the error only grows about 2% over $t = 50 M_{\text{ADM}}$. Notice that the smaller the value of q , the earlier the merger as indicated by t_{AH} in Table 1. Post-merger, the individual AHs lose their meaning as apparent horizons since by definition the AH denotes the *outermost* marginally trapped surfaces. The individual surfaces remain marginally trapped.

Fig. 2 shows snapshots of the horizons every $4.6 M_{\text{ADM}}$ before merger and at

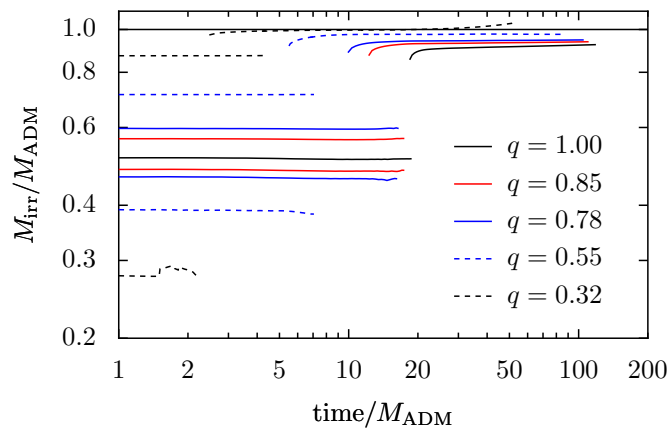


Figure 1. The irreducible mass of the apparent horizon as a function of time for different mass ratios q .

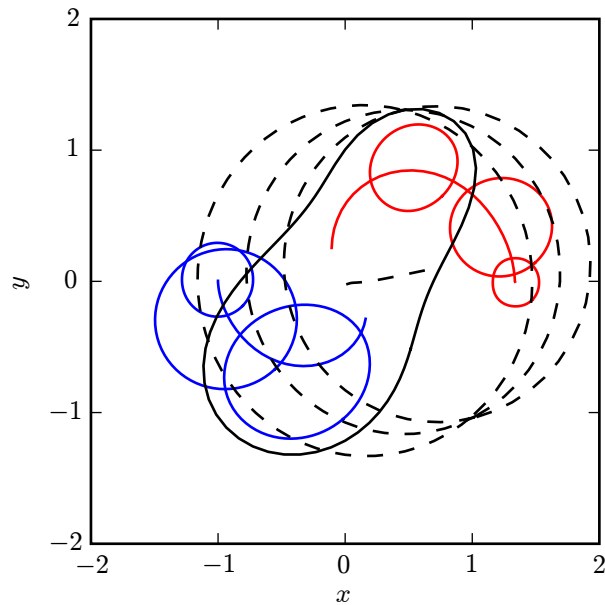


Figure 2. Snapshots of the AH location in the xy -plane for the case $q = 0.78$. The larger BH is on the left moving toward the bottom. The snapshots are taken every $4.6 M_{\text{ADM}}$ prior to merger and at $t = \{40, 80, 105\} M_{\text{ADM}}$ after merger. The first common AH is found at $t = 9.9 M_{\text{ADM}}$. The trajectories of the AH centroids are also shown. The common AH moves to the right and slightly upward after merger.

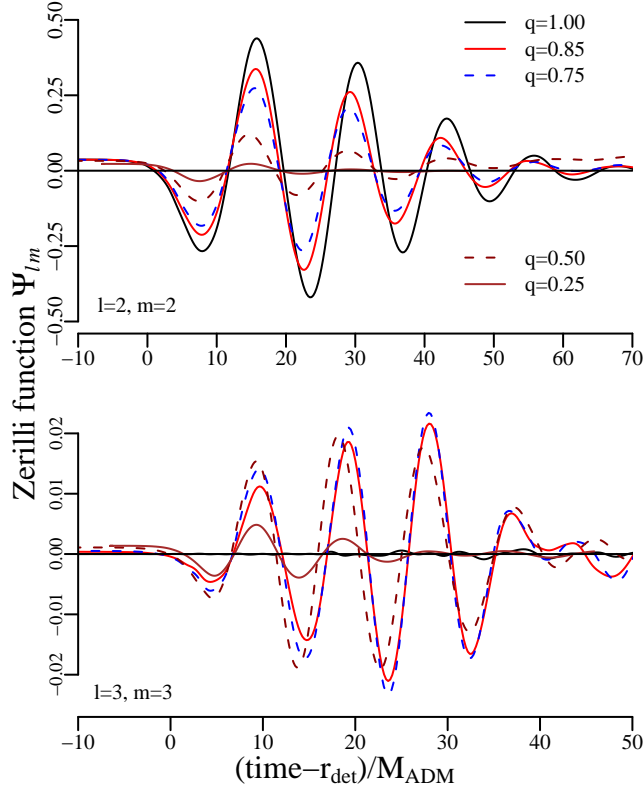


Figure 3. The dominant modes ($\ell = 2, m = 2$ and $\ell = 3, m = 3$) of the real part of the Zerilli function $\psi_{\ell m}$ against time for the different q ratios. The waveforms were extracted at $r = 15$. The $\ell = 2, m = 2$ mode decreases in amplitude with decreasing q while the $\ell = 3, m = 3$ mode increases and then decreases again.

$t = \{40, 80, 105\} M_{\text{ADM}}$ after merger for the $q = 0.78$ case. The other cases are qualitatively similar. Notice how the initial common AH has an asymmetric peanut shape due to the unequal masses. Soon after it appears, the common AH becomes spherical, as the dynamical gauges drive the coordinates toward those of a single BH. At that moment, the common AH begins to drift slowly away from the origin. The last AH snapshot in Fig. 2 was taken at $t = 105 M_{\text{ADM}}$. The evident drift in the coordinate location of the common AH provides a *hint* that a kick is generated as a consequence of gravitational recoil.

For waveform extraction, we compute Zerilli modes $\psi_{\ell m}$ using the Abrahams & Price convention [31]. Formally, the method assumes a spherically symmetric background. Simulations of QC-0 data [13, 14] have produced rotating BHs with Kerr parameter $a \sim 0.7$. The main effect of using Zerilli extraction in spacetimes with significant angular momentum content will be a spurious amplitude offset in the waveform [32, 33]. Fig. 3 displays the dominant modes ($\ell = 2, m = 2$ and $\ell = 3, m = 3$) for the different q simulations. The extraction surface is located at $r = 15$ with the outer boundary at $r = 96$. Notice in Fig. 3 that the $\ell = 2, m = 2$ mode simply decreases in amplitude as the q ratio is decreased. This is mostly due to the initial data approaching that of a single

q	E_{rad}	E_0	E_2	J_{rad}	V (km/s)
1.00	2.7 ± 0.8	0.05 ± 0.1	1.3 ± 0.4	15 ± 6	1 ± 2
0.85	1.7 ± 0.2	0.038 ± 0.004	0.78 ± 0.02	10 ± 0.8	50 ± 20
0.78	1.1 ± 0.8	0.06 ± 0.04	0.55 ± 0.02	7.4 ± 0.8	72 ± 40
0.55	0.4 ± 0.2	0.011 ± 0.006	0.16 ± 0.06	2.6 ± 0.6	90 ± 50
0.32	0.05	0.001	0.024	0.4	31

Table 2. Estimates of radiated energy E_{rad} (total), E_0 ($m = 0$ mode) and E_2 ($m = 2$ mode) as a % of the total initial ADM energy. Radiated angular momentum J_{rad} as a % of the initial angular momentum. Kick velocities V from gravitational recoil. The errors are the differences between the $h = 1/16$ and $1/20$ resolution results multiplied by 2.

distorted BH. The $\ell = 3, m = 3$ mode is smallest for the equal mass case (where it should be 0) and for the $q = 0.32$ case. Around $t = 50 M_{\text{ADM}}$, the lower amplitude waveforms become affected by outer boundary effects. The strongly dominant $\ell = 2, m = 2$ mode remains accurate until the end of the simulation except for the $q = 0.32$ case where even the dominant mode is affected by the boundary by $t = 60 M_{\text{ADM}}$.

From the extracted modes, Table 2 summarizes estimates of the energy E_{rad} and angular momentum J_{rad} emitted as % of the total energy and angular momentum as well as the recoil velocities V in km/s [34]. We compute the radiated energy from [31]

$$\frac{dE_{\text{rad}}}{dt} = \frac{1}{32\pi} \sum_{\ell, m} \left[\left| \frac{d\psi_{\ell m}^+}{dt} \right|^2 + |\psi_{\ell m}^\times|^2 \right], \quad (1)$$

the radiated angular momentum via

$$\frac{dJ_{\text{rad}}}{dt} = \frac{1}{32\pi} \sum_{\ell, m} im \left[\frac{d\psi_{\ell m}^+}{dt} (\psi_{\ell m}^+)^* + \psi_{\ell m}^\times \int_{-\infty}^t (\psi_{\ell m}^\times)^* dt' \right] \quad (2)$$

and the recoil velocity from

$$h_+ - ih_\times = \frac{1}{\sqrt{2}r} \sum_{\ell, m} \left[\psi_{\ell m}^+ - i \int_{-\infty}^t \psi_{\ell m}^\times dt' \right] {}_{-2}Y^{\ell m}(\theta, \phi)$$

$$\frac{dP^k}{dt} = \frac{r^2}{16\pi} \int \left[\left(\frac{dh_+}{dt} \right)^2 + \left(\frac{dh_\times}{dt} \right)^2 \right] n^k d\Omega.$$

Here ${}_{-2}Y^{\ell m}(\theta, \phi)$ denotes the spin-weight -2 tensor spherical harmonics. The kick velocity is obtained from $M V^i = \int P^i dt$ with M the total mass of the binary. The reported recoil velocity is $|V|$.

As expected, the radiated energy and angular momentum are strongly dominated by the $\ell = 2, m = 2$ mode. The energy and angular momentum radiated for the $q = 1$ case are in good agreement with previous work [14, 13]. The numbers reported in the table are computed from the $h = 1/20$ simulations. The errors are the difference between the quantities computed from the $h = \{1/16, 1/20\}$ resolution simulations multiplied by 2. The Richardson error estimate for our resolutions and 2nd order

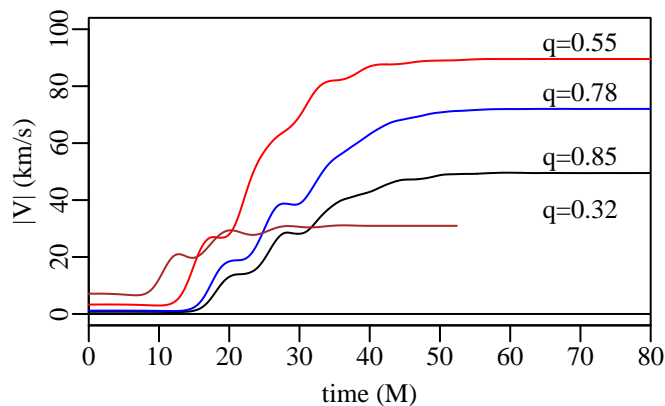


Figure 4. Recoil velocity accumulated against time for the different models. Note that in comparison to far separated inspiral models ([36, 18]) the inspiral contribution is missing. Also the $q = 0.32$ case shows an initial offset from zero which comes from the too close extraction radius.

convergence is $16/9$ and 2 is used as a conservative bound. We do not report errors for the $q = 0.32$ because the $h = 1/16$ simulation has insufficient resolution to compute the waveform. With increasing resolution the estimates of E_{rad} and J_{rad} did increase, so assuming convergence, one would expect the continuum estimates for radiated energies and angular momenta to be slightly higher than those reported here.

In order to compare the gravitational wave content of different simulations, Table 2 also presents the energy emitted in the $m = 0$ and $m = 2$ modes, i.e. E_0 and E_2 respectively, as a % of the total initial ADM energy. The $\ell = 2, m = 0$ waveform in the $q = 1$ case changes quite strongly between the $h = 1/20$ and $h = 1/16$ simulations, resulting in large error bars on E_0 and V (which should be zero for the equal mass case). Since the effect is not as strong for the $\ell = 2, m = 2$ mode, the dominant mode for E and J_{rad} , the error bars are smaller. The $\ell = 2, m = 2$ mode dominates for a pure inspiral, whereas the $\ell = 2, m = 0$ mode dominates for a plunge, so we would expect a larger E_2/E_0 ratio for inspirals than for plunges. It is reassuring that differences in the radiated energies of these modes exist; however, due to the construction of the initial data sequence, these differences do not reflect a change of q only. It will be interesting to see how this changes with further separated, truly inspiraling configurations starting from outside ISCO.

The recoil velocities, V , reported in Table 1 are consistent with those obtained from head-on collisions [37], mixed numerical-perturbative inspiral mergers [35] and recent fully relativistic results at larger separations [36, 18]. For reference, kicks from gravitational recoil of relevance to galactic BH merger scenarios [9] have been recently estimated to second post-Newtonian order [16]. The kicks were found to be dominated by the plunge phase and could reach speeds larger than 100 km/s for $0.1 \leq \eta \leq 0.24$ or $1/8 \leq q \leq 2/3$. Recent work using the effective one-body approach gives lower kick velocities of at most 74 km/s at $\eta = 0.2$ or $q = 0.38$ [17].

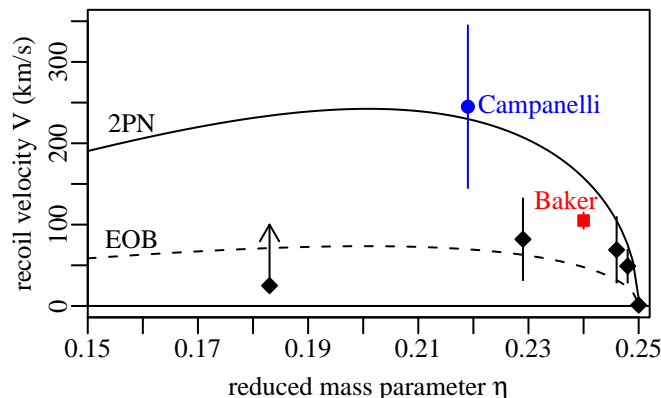


Figure 5. A comparison of recoil velocity estimates as a function of η . The 2PN estimates of Blanchet et al. [16] are denoted by the solid line and those from Gopakumar-Damour [17] by a dashed line. Campanelli [35] and Baker et al. [36] kicks are labeled by a circle and a box, respectively, and our recoil velocities are labeled with diamonds. Note that the smaller η cases present lower bounds due to the initial data configurations studied.

In Fig. 4 we show the recoil velocity accumulated as a function of time. The close detector radius manifests itself in the non-zero initial offset of the recoil velocity of the $q = 0.32$ model. The inspiral contribution is notably absent from these models due to their close separation (compare Refs.[36, 18]). Also note that the initial data contains an initial feature that we cannot remove as it is already overlaid with the merger signal. In further separation models as in Ref. [18] the initial feature shows up in the weaker inspiral part and can therefore easily be removed. Fig. 5 shows our recoil velocities as a function of the reduced mass parameter η , including kick estimates found by others [16, 17, 35, 36]. Our $q = 0.85$, $\eta = 0.248$ and $q = 0.78$, $\eta = 0.246$ cases are comparable to the estimates from Blanchet et al. [16]. The reason for the agreement is that these cases are closer to the QC-0 equal mass case. Thus the initial data setup is not too far from ISCO and quasi-circularity. The case $q = 0.55$, $\eta = 0.229$ yields the largest recoil velocity, ~ 82 km/s, also consistent with Blanchet et al. [16] who find a peak in the recoil around $q = 0.4$, $\eta = 0.204$. Recently Baker et al. [36] reported a recoil velocity of 105 km/s for $q = 0.67$, $\eta = 0.24$, a value larger than our kicks. The difference is mostly due to the larger initial separation of their BHs. Our smallest kick is obtained in the $q = 0.32$, $\eta = 0.183$ case. This is likely a significant underestimation since we are probably dealing with a *single* distorted BH.

Conclusions. We have shown results from a series of unequal mass BBH inspiral simulations. The kick velocities spanned a range of 25-82 km/s. Our kick velocity estimates should be understood as a lower bound because the initial separations are smaller than those normally used (for example in Ref. [16]) for the plunge phase. The observed drop in the time to merger t_{AH} in our results comes from our approach in which the angular momentum of the configuration decreases as the bare mass ratio is decreased. This approach introduces significant uncertainty in the recoil extracted and

in particular it is possible that for our cases with $q \leq 0.55$, a common event horizon already exists in the initial data slice; and, therefore, we are evolving a single, distorted BH. Ideally one would like to compare initial data sets which are far separated and have the same orbital frequency. We would also like to point out that these close configurations contain significant eccentricities which are known to influence the recoil velocities. For small eccentricities $e \leq 0.1$ Ref. [2] shows $V_R \propto (1 + e)$. More on equal mass inspirals and eccentricities can be found in Ref. [38, 39].

In addition to the gravitational recoil, we estimated the radiated energy and angular momentum, paying particular attention at the energy radiated independently in the $m = 0, 2$ modes. We also monitored the irreducible masses during the simulations, providing a good indicator that the near-zone physics was accurately evolved. A more detailed comparison of the dependence of the waveforms on the mass ratio from inspirals starting outside the ISCO is currently under investigation. A strong dependence of the waveform on the binary parameters would facilitate their estimation, but at the same time it would hinder initial detection efforts as many templates would be required. If waveforms, on the other hand, do not vary significantly with mass ratios, the search effort could be easier at the expense of accurate parameter estimation.

Acknowledgments. We thank E. Schnetter, M. Ansorg and J. Thornburg for providing access to π -symmetry, initial data and AH infrastructure, respectively, and U. Sperhake and C. Sopuerta for helpful discussions. Simulations performed at the CGWP, AEI, CCT, LRZ, NCSA, NERSC, PSC, PSU and RZG. The Center for Gravitational Wave Physics is supported by the NSF under cooperative agreement PHY-0114375. Work partially supported by NCSA grant MCA02N014 and NSF grants PHY-0244788, PHY-0354821. PL and DS thank the hospitality of KITP, supported by NSF PHY-9907949.

References

- [1] C. F. Sopuerta, N. Yunes, and P. Laguna. Gravitational recoil from binary black hole mergers: The close-limit approximation. *Phys. Rev. D*, 74:124010, 2006
- [2] C. F. Sopuerta, N. Yunes, and P. Laguna. Gravitational recoil velocities from eccentric binary black hole mergers. *Astrophys. J.*, 656:L9-L12, 2007
- [3] K. Danzmann. LISA - An ESA cornerstone mission for the detection and observation of gravitational waves. *Advances in Space Research*, 32:1233–1242, October 2003.
- [4] T. Prince. LISA: The Laser Interferometer Space Antenna. In *Bulletin of the American Astronomical Society*, 35:751, May 2003.
- [5] D. Richstone, E. A. Ajhar, R. Bender, G. Bower, A. Dressler, S. M. Faber, A. V. Filippenko, K. Gebhardt, R. Green, L. C. Ho, J. Kormendy, T. R. Lauer, J. Magorrian, and S. Tremaine. Supermassive black holes and the evolution of galaxies. *Nature*, 395:A14+, October 1998.
- [6] John Magorrian et al. The demography of massive dark objects in galaxy centres. *Astron. J.*, 115:2285, 1998.
- [7] J. D. Bekenstein. Gravitational-Radiation Recoil and Runaway Black Holes. *Ap. J. Lett.*, 183:657–664, July 1973.
- [8] P. Madau and E. Quataert. The Effect of Gravitational-Wave Recoil on the Demography of Massive Black Holes. *Ap. J. Lett.*, 606:L17–L20, May 2004.

- [9] David Merritt, Milos Milosavljevic, Marc Favata, Scott A. Hughes, and Daniel E. Holz. Consequences of gravitational radiation recoil. *Astrophys. J.*, 607:L9–L12, 2004.
- [10] Bernd Brügmann, Wolfgang Tichy, and Nina Jansen. Numerical simulation of orbiting black holes. *Phys. Rev. Lett.*, 92:211101, 2004.
- [11] Miguel Alcubierre, Bernd Brügmann, Peter Diener, Francisco Siddhartha Guzmán, Ian Hawke, Scott Hawley, Frank Herrmann, Michael Koppitz, Denis Pollney, Edward Seidel, and Jonathan Thornburg. Dynamical evolution of quasi-circular binary black hole data. *Phys. Rev. D*, 72:044004, 5 August 2005.
- [12] Frans Pretorius. Evolution of binary black hole spacetimes. *Phys. Rev. Lett.*, 95:121101, 2005.
- [13] Manuela Campanelli, C. O. Lousto, P. Marronetti, and Y. Zlochower. Accurate evolutions of orbiting black-hole binaries without excision. *Phys. Rev. Lett.*, 96:111101, 2006.
- [14] John G. Baker, Joan Centrella, Dae-Il Choi, Michael Koppitz, and James van Meter. Gravitational wave extraction from an inspiraling configuration of merging black holes. *Phys. Rev. Lett.*, 96:111102, 2006.
- [15] Peter Diener et al. Accurate evolution of orbiting binary black holes. *Phys. Rev. Lett.*, 96:121101, 2006.
- [16] Luc Blanchet, Moh'd S. S. Qusailah, and Clifford M. Will. Gravitational recoil of inspiralling black-hole binaries to second post-newtonian order. *Astrophys. J.*, 635:508, 2005.
- [17] Thibault Damour and Achamveedu Gopakumar. Gravitational recoil during binary black hole coalescence using the effective one body approach. *Phys. Rev. D*, 73(12):124006, 2006.
- [18] Jose A. Gonzalez, Ulrich Sperhake, Bernd Brügmann, Mark Hannam, and Sascha Husa. Maximum Kick from Nonspinning Black-Hole Binary Inspiral. *Phys. Rev. Lett.* 98(9):091101, 2007.
- [19] S. Brandt and B. Brügmann. A simple construction of initial data for multiple black holes. *Phys. Rev. Lett.*, 78(19):3606–3609, 1997.
- [20] Marcus Ansorg, Bernd Brügmann, and Wolfgang Tichy. A single-domain spectral method for black hole puncture data. *Phys. Rev. D*, 70:064011, 2004.
- [21] Miguel Alcubierre, Bernd Brügmann, Peter Diener, Michael Koppitz, Denis Pollney, Edward Seidel, and Ryoji Takahashi. Gauge conditions for long-term numerical black hole evolutions without excision. *Phys. Rev. D*, 67:084023, 2003.
- [22] J. Baker, M. Campanelli, C. O. Lousto, and R. Takahashi. Modeling gravitational radiation from coalescing binary black holes. *Phys. Rev. D*, 65:124012, 2002.
- [23] G. B. Cook. Three-dimensional initial data for the collision of two black holes. II. Quasicircular orbits for equal-mass black holes. *Phys. Rev. D*, 50:5025–5032, October 1994.
- [24] Takashi Nakamura, Ken-ichi Oohara, and Y. Kojima. General relativistic collapse to black holes and gravitational waves from black holes. *Prog. Theor. Phys. Suppl.*, 90:1–218, 1987.
- [25] M. Shibata and Takashi Nakamura. Evolution of three-dimensional gravitational waves: Harmonic slicing case. *Phys. Rev. D*, 52:5428, 1995.
- [26] Thomas W. Baumgarte and Stuart L. Shapiro. On the numerical integration of Einstein's field equations. *Phys. Rev. D*, 59:024007, 1999.
- [27] Sascha Husa, Ian Hinder, and Christiane Lechner. Kranc: a mathematica application to generate numerical codes for tensorial evolution equations. *Computer Physics Communications*, 174:983–1004, 2006.
- [28] Erik Schnetter, Scott H. Hawley, and Ian Hawke. Evolutions in 3D numerical relativity using fixed mesh refinement. *Class. Quantum Grav.*, 21(6):1465–1488, 21 March 2004.
- [29] Jonathan Thornburg. A fast apparent-horizon finder for 3-dimensional Cartesian grids in numerical relativity. *Class. Quantum Grav.*, 21(2):743–766, 21 January 2004.
- [30] James R. van Meter, John G. Baker, Michael Koppitz, and Dae-Il Choi. How to move a black hole without excision: gauge conditions for the numerical evolution of a moving puncture. *Phys. Rev. D.*, 73(12):124011, 2006.
- [31] A. Nagar and L. Rezzolla. TOPICAL REVIEW: Gauge-invariant non-spherical metric

- perturbations of Schwarzschild black-hole spacetimes. *Class. Quantum Grav.*, 22:167, August 2005.
- [32] M. Alcubierre, W. Bengert, B. Brügmann, G. Lanfermann, L. Nergel, E. Seidel, and R. Takahashi. 3D Grazing Collision of Two Black Holes. *Phys. Rev. Lett.*, 87(26):271103, December 2001.
- [33] Steven R. Brandt and Edward Seidel. The evolution of distorted rotating black holes. 2: Dynamics and analysis. *Phys. Rev.*, D52:870–886, 1995.
- [34] Alan G. Wiseman. Coalescing binary systems of compact objects to (post)5/2 newtonian order. 2. higher order wave forms and radiation recoil. *Phys. Rev. D*, 46:1517–1539, 1992.
- [35] M. Campanelli. Understanding the fate of merging supermassive black holes. *Class. Quantum Grav.*, 22:387, May 2005.
- [36] John G. Baker et al. Getting a kick out of numerical relativity. *Astrophys. J.*, 653:L93-L96, 2006.
- [37] Peter Anninos and S. Brandt. Head-on collision of two unequal mass black holes. *Phys. Rev. Lett.*, 81:508–511, 1998.
- [38] A. Buonanno, G. B. Cook, F. Pretorius. Inspiral, merger and ring-down of equal-mass black-hole binaries gr-qc/0610122
- [39] Harald P. Pfeiffer et al. Reducing orbital eccentricity in binary black hole simulations gr-qc/0702106